J. exp. Biol. **162**, 1–21 (1992)
Printed in Great Britain © *The Company of Biologists Limited 1992*

HYDROID STOLONAL CONTRACTIONS MEDIATED BY CONTRACTILE VACUOLES

BY B. SCHIERWATER[1], B. PIEKOS[1] AND L. W. BUSS[1,2]

[1]*Department of Biology* and [2]*Department of Geology and Geophysics, Yale University, New Haven, CT 06511, USA*

Accepted 16 April 1991

Summary

The growth and development of colonial hydroids is dependent upon a flow of gastrovascular fluid through a common vasculature. Gastrovascular flow is believed to be driven by polyp contractions, stolonal contractions and endodermal ciliation. In the athecate hydroid *Hydractinia symbiolongicarpus* we found that polyp contractions, stolonal contractions and gastrovascular flow were only weakly correlated on a local scale. Stolons isolated from vascular continuity to polyps were found to display contraction frequencies indistinguishable from those observed in intact colonies. Transmission electron micrographs reveal a unique organelle, with characteristics of a contractile vacuole, in the apical stolonal endoderm. The activity of this organelle, inferred from static observations, correlates with the observed pattern of stolonal contractions. This is the first record of a contractile vacuole in an eumetazoan animal. Its description calls for a revision of existing interpretations of the mechanism of stolonal contractions in hydroids.

Introduction

In Hydrozoa, and in particular hydroids, a colonially organized polyp generation is the most frequent or even the only generation to develop. The development of a colony starts with the metamorphosis of an actinula or planula larva into a primary polyp, which grows a primary stolon. This stolon can grow and bifurcate in a variety of ways, resulting in different types of two- and three-dimensional colony growth forms. The morphological subunits of developing colonies, however, share a common organizational plan (see Fig. 1A). Polyps, which serve as feeding organs, are connected to one another by tubular extensions of a common gastrovascular cavity to form a stolonal vasculature. The vasculature bathes tissues in a common gastrovascular fluid, the movement of which is presumed to be driven by some combination of polyp contractions, stolon contractions and endodermal ciliation (Hauenschild, 1954; Crowell, 1974; Müller,

Key words: contractile vacuole, endoderm, ultrastructure, gastrovascular flow, hydroids, stolon contraction, stolonal growth, *Eleutheria dichotoma*, *Hydractinia symbiolongicarpus*.

1974). Colonies grow by elongation of stolon tips, by induction of new tips and by vegetative iteration of new polyps along these stolons (Müller *et al.* 1987).

Although the importance of gastrovascular flow for hydroid growth and development is unquestioned (Hauschka, 1944; Berrill, 1949; Hauenschild, 1954; Hale, 1960; Fulton, 1963; Karlson and Marferin, 1984; Marferin, 1985; Müller *et al.* 1987), the contribution of stolonal contractions to these processes remains unclear. Three views are evident in the literature. Berrill (1949), Hale (1960, 1964), Fulton (1963), Hudson (1965) and Donaldson (1974) have suggested that gastrovascular flow is driven by specialized contractile regions that occur in some thecate hydroids just proximal to stolon tips, whereas Hauenschild (1954), Crowell (1974) and Müller (1974, 1975) have suggested that a combination of polyp contractions, stolonal contractions and endodermal ciliation drive gastrovascular flow. Marferin (1985), however, regards stolonal contractions to be an incidental by-product of gastrovascular flow driven by polyp contractions. Of these divergent views, only the relationship between gastrovascular flow and endodermal ciliation has been determined. Experiments performed by Berrill (1949) and Hale (1964) have shown that gastrovascular flow ceases under conditions in which stolonal and polyp contractions are blocked, but endodermal ciliation remains unaltered. Our relative lack of understanding of the forces governing gastrovascular flow is unfortunate in that patterns of gastrovascular flow within colonies are highly stereotyped in both growing (Karlson and Marferin, 1984; Marferin, 1985) and regenerating (Huxley and deBeer, 1923; Hammett and Padis, 1935; Hale, 1964) animals, suggesting the existence of sophisticated mechanisms governing its distribution.

Using the athecate hydroid *Hydractinia symbiolongicarpus* (Buss and Yund, 1989), we (i) quantify stolon contraction rates under various conditions of feeding, starvation and temperature; (ii) show by experimental manipulation that stolon contractions occur at normal frequencies in the absence of polyps, raising the question of the origin of stolonal contractions; and (iii) present micrographic studies that reveal the presence of a contractile vacuole in the stolon endoderm whose activity correlates with the observed pattern of stolonal contractions.

Materials and methods

Animals

Clonal propagations of two *Hydractinia symbiolongicarpus* colonies were used for all experiments. Both clones were highly stoloniferous ('net type', Hauenschild, 1954). Clone α (male) was a field-collected colony from Long Island Sound (Guilford, CT); while clone β (female) was derived from a mating of two field-collected colonies. Stock colonies were maintained on hermit crab shells in 40-l recirculating aquaria at 16°C and fed 3- to 4-day-old nauplii of *Artemia salina* daily. Clonal propagations were established by standard methods (McFadden *et al.* 1984). Clonal explants were grown on 22 mm×40 mm cover slips for video microscopy and actin staining. Explants for transmission electron microscopy

(TEM) were grown in Falcon Petri dishes (25 mm). All clonal explants were maintained at 21–23 °C and fed every 2 days with 4- to 5-day-old nauplii reared at 16 °C. All experimental colonies were in a non-reproductive state and bearing feeding polyps (hereafter referred to as polyps) as the only type of hydranth. These colonies were kept under artificial daylight conditions of L:D 16 h:8 h between experiments and under constant light conditions (L:D 24 h:0 h) throughout the experiments. In addition, colonies of the athecate hydroid *Eleutheria dichotoma* Quatrefagos, were cultured in a similar manner (Hauenschild, 1956) for the purpose of comparative TEM studies on the ultrastructure of the stolons.

Video microscopy

Colonies on cover slips were mounted in a silicon rubber-coated aluminum chamber (110 mm×40 mm×15 mm) with a circular hole (16 mm diameter) in the bottom, allowing the microscope objectives to contact the cover slips from underneath the colony. The animal chamber was thermoregulated by using a constant-temperature stage (Rainin, Massachusetts, model 5000 digital controller, model 5002 slide holder), allowing temperature constancy to better than ±1 °C. Stolons were videotaped using a Zeiss Axiovert 35 microscope either in bright field (2.5× Plan-Neofluar) or differential interference contrast (DIC) (20× and 40× Achroplane), with or without a 1.6× magnifier. The microscope was equipped with a phototube interfaced to a Dage MTI 70 series camera, Mitsubishi time-lapse video cassette recorder HS-480U, Mitsubishi video copy processor P61U, and a high-resolution Panasonic WV5410 black and white monitor. For measuring the time course of changes in stolon canal diameter during contraction–expansion cycles, the video recorder was interfaced with a microcomputer (IBM-compatible PC-AT) equipped with the Bioscan Optimas image-analysis software. 35 mm micrographs were obtained using a Nikon F3 HP camera body and Kodak T-MAX professional 100 ASA black and white film.

Stolon contraction rates as a function of temperature

The effect of temperature on the rate of stolon contraction was quantified at two different sites, S0 (i.e. a main stolon bearing a feeding polyp) and S1 (i.e. a side branch without a polyp), within intact colonies, as shown in Fig. 1B. S0 and S1 stolons of clones α and β were videotaped at 60× time lapse while temperature was raised continuously from 5 to 31 °C over a period of 12 h. The number of stolon contractions per 30 min interval was counted and plotted against the actual temperature at the beginning of the interval. The frequency of stolonal contraction was measured a day before and a day after the experiment at 18 °C for each experimental colony. Only those colonies that showed no significant effect of experimental manipulation on contraction rates were utilized in the analysis. Different linear and non-linear regression models were tested to fit the data using SAS and BMDP, and a decision on the best fit was based on the deviation values for the residual sums of squares (RSS) (Schierwater, 1989).

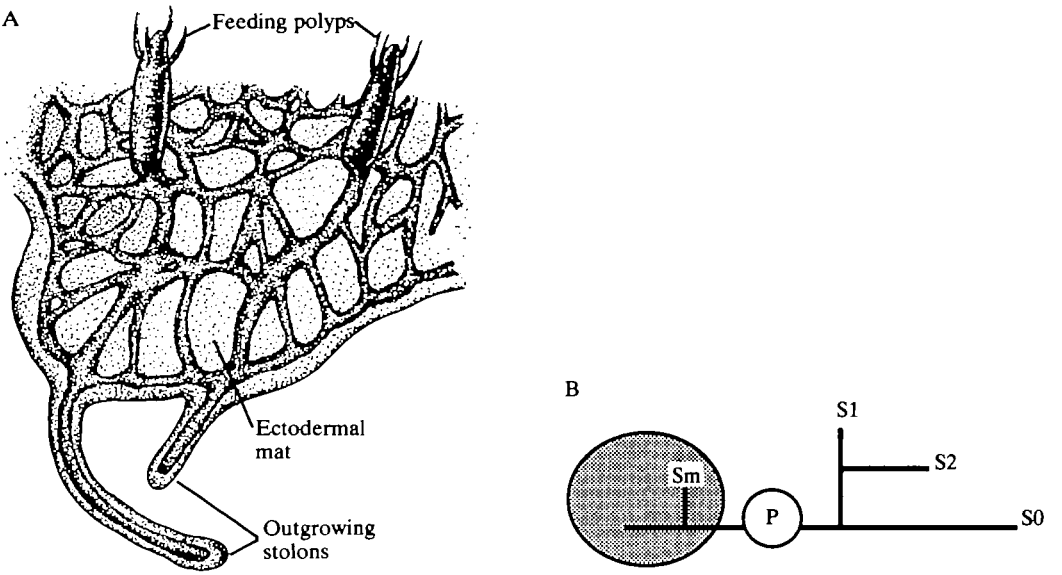

Fig. 1. (A) Portion of a *Hydractinia symbiolongicarpus* colony with two feeding polyps, an ectodermal mat and two outgrowing stolons (approx. 32×). (B) Abbreviations used in the text for describing the different regions of the stolons tested: Sm, any stolon inside the ectodermal stolonal mat of a colony; S0, stolon bearing a feeding polyp (P); S1, side branch of S0, which bears no feeding polyp and, therefore, is one branching event away from the next feeding polyp; S2, stolon that is two branching events away from the next feeding polyp.

Simultaneous quantification of stolon contraction, polyp contraction and gastrovascular flow

The relationship between stolon contraction, polyp contraction and the direction of gastrovascular flow was investigated by simultaneous monitoring of all three variables in an intact growing colony. As above, two different sites (S0, S1) in each of the two clones (α, β) were observed. Stolons were videotaped at 60× time lapse and at about 200× final magnification on the screen. At 22°C each colony was starved for 24 h, monitored for 24 h, then fed and monitored again for a further 24 h. Using a simultaneous on-screen monitoring of time, tapes were analyzed to obtain the number of stolonal contractions, the number of changes in the direction of the gastrovascular flow and the number of contractions of the polyp for hourly intervals. Nonparametric Kendall's tau correlations were calculated for all the listed variables using BMDP. It is important to emphasize that these measures are only capable of revealing correlations between local events. The field of view was limited to a total area of approximately 1.5 mm^2 of the colony appearing on the screen and the influence of patterns of polyp or stolonal contractions outside this limited region of the colony will not be revealed by these methods.

Contractions in isolated stolons

To determine whether stolon contractions persist in the absence of direct vascular connection to polyps, we severed the connections between a segment of stolon and the colony. Isolated segments of stolons, ranging in length from 200 to 500 μm, were produced in four regions of colonies of clone α: S0, S1, S2 and Sm (see Fig. 1). An additional eight stolons, four S0 and four S1, of clone β were tested in the same way. Stolon contraction rates were quantified by video microscopy as described above for a 2 h period prior to surgery and a 10 h period after surgery. Stolon contraction rates before and after surgery were compared using a Mann–Whitney *U*-test (two-tailed).

Transmission electron microscopy

Stolons of both clones, α and β, were examined using TEM to determine whether characteristic intracellular changes accompanied stolonal contractions. Samples were observed in each of three possible states: fully contracted, fully expanded and in transition between contracted and expanded. Stolons of 500 μm length were severed from the mother colony, microvideotaped for 1 h, and fixed in glutaraldehyde as soon as the different contraction stages were found simultaneously along the stolon. Photographs of the stolon were taken at the moment of fixation and subsequently used as a guide for cross sections analysed by TEM. Colonies were fixed for 1 h in 4 % glutaraldehyde (prepared in artificial sea water 'Instant Ocean', pH 7.4), washed in Instant Ocean, and post-fixed for 1 h in 1 % osmium tetroxide. Colonies were then dehydrated in a graded series of ethanol washes and embedded in Spurr's epoxy resin. Semi-thin sections (1 μm) were cut with a Sorvall MT-2 ultramicrotome, mounted on glass slides, and stained with Toluidine Blue. Ultrathin sections from silver to gray interference color were cut with a diamond knife, stained with uranyl acetate and lead citrate, and viewed on either a Philips 300 or a Zeiss EM-10 TEM. For strictly qualitative comparisons, stolons from *Eleutheria dichotoma* were also examined by TEM.

The relative contributions of changes in the volume of ectodermal and endodermal vacuoles to a stolonal contraction were estimated from electron micrographs. The point-counting method (1 cm×1 cm grid, final magnification 6700×) was used to estimate the fractional vacuolar volume (ratio of vacuole volume to total volume) of both the endoderm and ectoderm. The same grid was used to estimate cytoplasmic area when determining the density of zipper-like organelles (ZLOs) (see Results, final magnification 50 000×).

Rhodamine–Phalloidin staining

Rhodamine–Phalloidin was utilized to visualize F-actin in intact stolons (Faulstich *et al.* 1988). Explants were established on cover slips and grown for a period of 3–4 weeks, by which time they had reached a size of 5–10 feeding polyps with 4–5 branched peripheral stolons. Whole colonies were fixed for 5 min in 2 % paraformaldehyde in phosphate-buffered saline (PBS), rinsed once in PBS, and

quenched for 5 min to 50 mmol l^{-1} NH_4Cl, and then incubated in the dark for 5 min with Rhodamine–Phalloidin (Molecular Probes, Eugene, Oregon, no. R415; 1:50 in 1 % Triton X-100 in PBS). The colonies were then washed three times with PBS and mounted with 100 mmol l^{-1} *n*-propyl gallate in 50 % glycerol–PBS, to prevent bleaching. The material was viewed at once, using a Zeiss microscope equipped with a 63× Planapo oil-immersion objective, for both phase and epifluorescence viewing. Micrographs were made with an Olympus OM-2 camera body using Kodak T-MAX professional 400 ASA black and white film, exposed and developed for 1600 ASA.

Results

Characterization of stolon contractions

A complete stolon contraction cycle consists of the contraction phase, during which the canal closes, and an expansion phase, during which the canal reopens (see Fig. 2). In Fig. 3A the time course for a series of five consecutive complete contraction–expansion cycles is shown for a temperature of 25 °C. The time for the stolon contraction phase (mean ±1 S.E., 54.7±4.68 s) was significantly longer than for the expansion phase (39.8±4.45 s) ($P<0.05$, Wilcoxon, two-tailed). The uneven distribution of the speed at which the canal is closed and reopened is shown in Fig. 3B. This limit cycle uses the same data as the stolon contraction–expansion periodicity in Fig. 3A.

Effects of temperature on stolon contractions

The rate of stolon contraction (i.e. the number of complete contraction–expansion cycles per hour) bears a sigmoid relationship to temperature for all stolons tested. The pooled values for the different clones (α and β) and positions within colonies (S0 and S1) are shown in Fig. 4. A sigmoid regression curve was found to display a more than 13 % better fit to the data than any linear or simple exponential regression model. The means±S.D. for the three estimated variables of the best fitting sigmoid regression given in Fig. 4 are 57.4±5.09, 1.3±0.53, 0.178±0.024; RSS=388, d.f.=75. Two aspects of this relationship are noteworthy. First, the range over which stolon contraction rates are most sensitive to temperature (15–25 °C) is within the range of summertime temperatures experienced by these organisms (Buss and Yund, 1988), whereas the extremes of temperature lie outside the range of values naturally encountered by growing colonies. Second, this function is characteristic of that obtained for active, temperature-dependent metabolic processes (Precht at *al.* 1973; Cossins and Bowler, 1987). The average Q_{10} value in the temperature range between 15 and 25 °C is 2.7 (calculated from the regression). It should be noted that the absolute values for the contraction frequencies might be underestimates, because of the possibility of a delayed physiological response to temperature changes. The

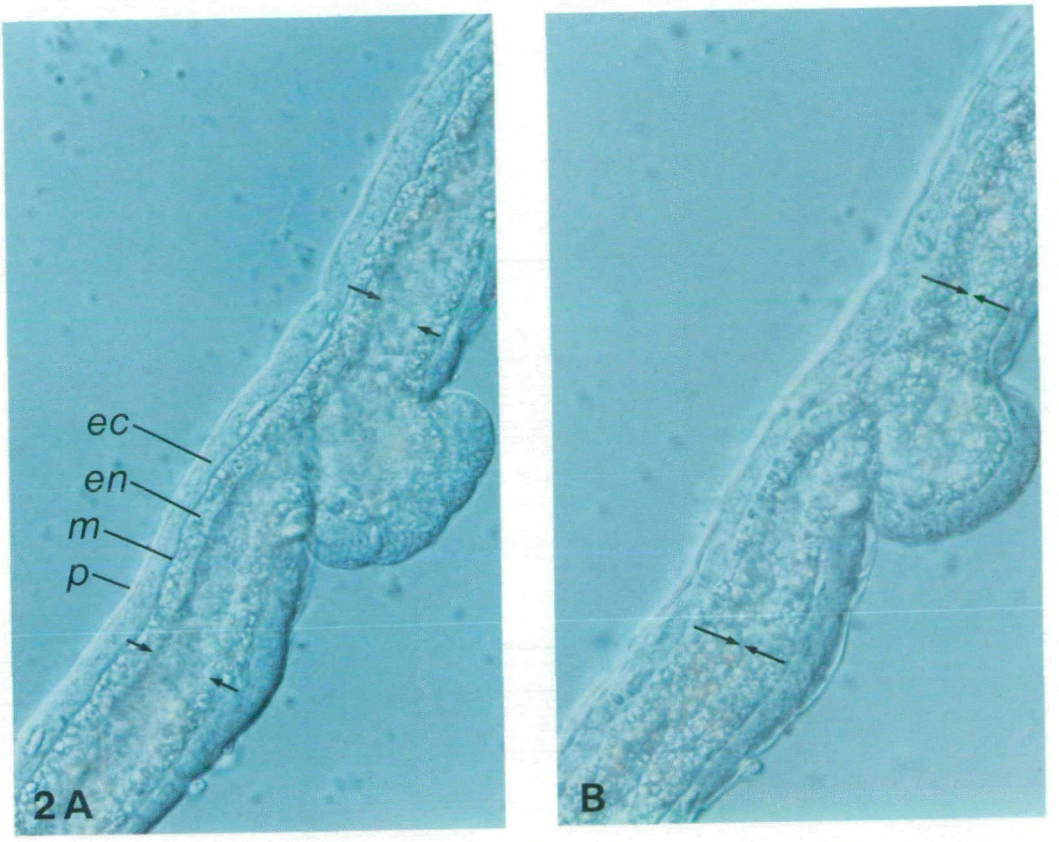

Fig. 2. Differential interference contrast photograph of a stolon of *Hydractinia symbiolongicarpus* at an expanded (A) and a largely contracted (B) stage. *ec*, ectoderm; *en*, endoderm; *m*, mesoglea; *p*, periderm; the head-to-head arrows mark the thickness of the endoderm and hence the space between the two arrowheads marks the diameter of the open stolonal canal. The diameter of the expanded canal is 40 μm.

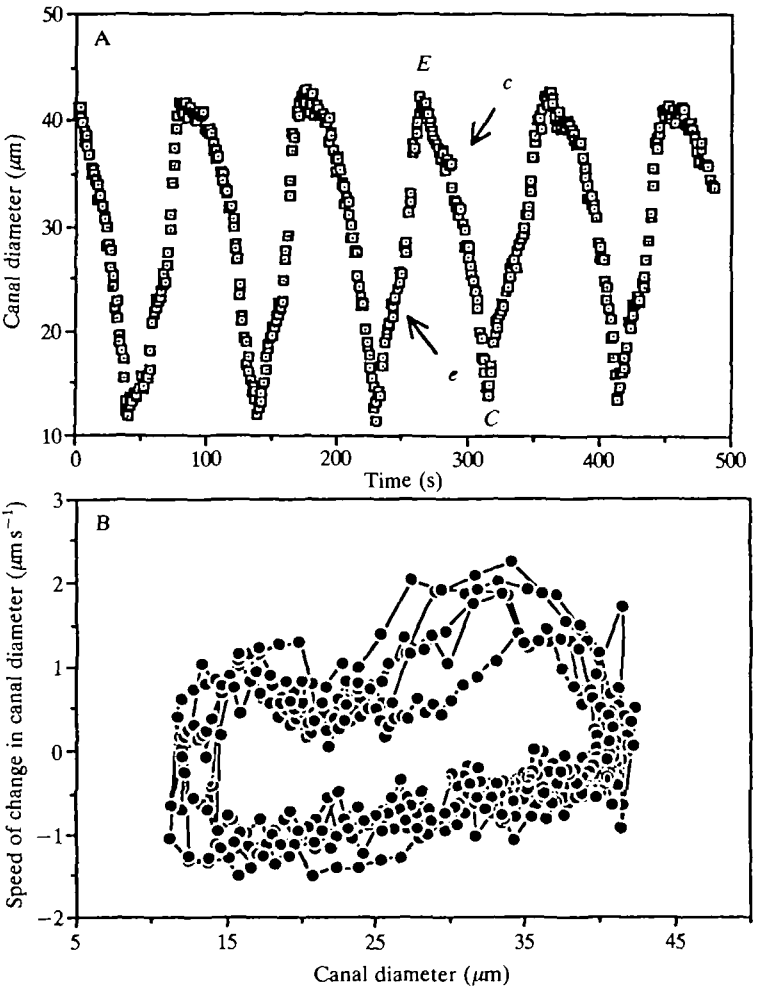

Fig. 3. (A) Time course of five complete stolon contraction–expansion cycles at 25 °C. 495 consecutive measurements at 1 s intervals of the canal diameter are plotted. The situations of a fully expanded and a fully contracted stolon are marked with *E* (expanded) and *C* (contracted). The slopes for the increase in canal diameter (marked *e* for expansion phase) are significantly steeper than the slopes for decreasing canal diameters (*c*, contraction phase), i.e. the stolon expands significantly faster than it contracts ($P<0.05$, Wilcoxon, two-tailed test). (B) The limit cycle for the expansion–contraction periodicity, as derived from a four-point smoothing of the data presented in A. The speed of changes in canal diameter is plotted against the canal diameter. Note the obvious differences in the speeds for closing the canal (stolon contraction, negative values in the figure) and opening the canal (stolon expansion, positive values) and the uneven accelerations at different stages in the contraction–expansion cycle. The highest speeds (of about 2 $\mu m\,s^{-1}$) are found in the last half of the stolon expansion phase.

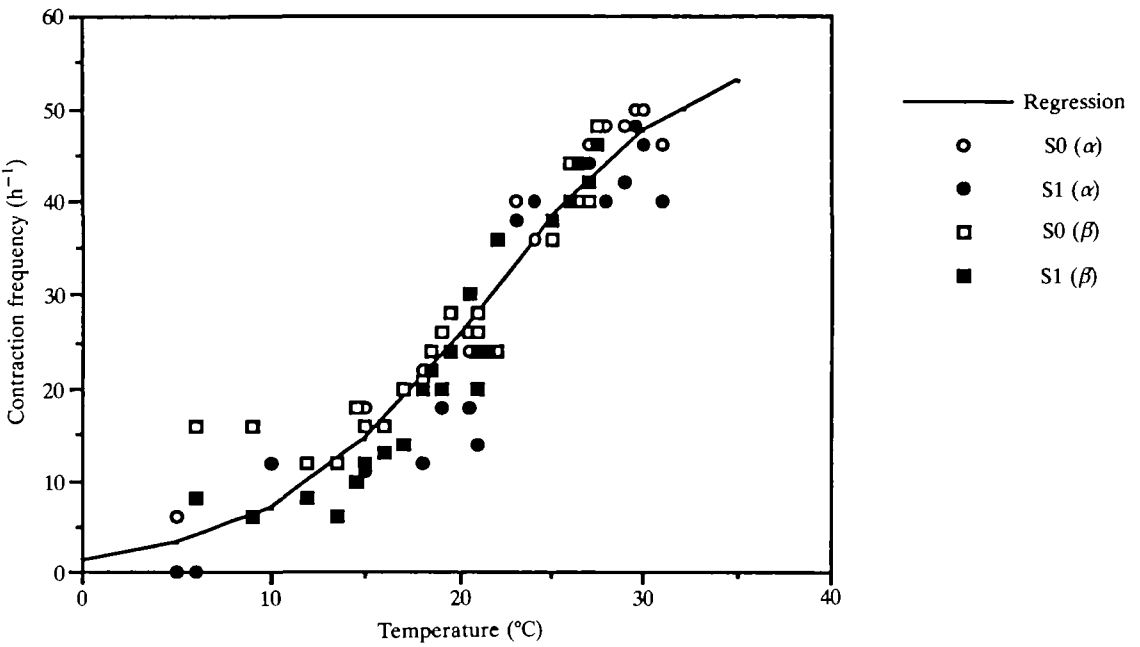

Fig. 4. Temperature dependence of stolon contraction frequency in *Hydractinia symbiolongicarpus*. Results are plotted for four different stolons from two clones (N=76). The best fitting regression curve is sigmoid. The region of exponential increase is found in the biologically most relevant temperature range between 15 and 25°C. The equation for the curve is: $y=57.4\times1.3e^{0.178x}/(57.4-1.3+1.3e^{0.178x})$.

sigmoid shape of the regression and the slope (Q_{10} values), however, would not be affected.

Polyp contractions, stolonal contractions and gastrovascular flow

A correlation matrix of stolon contraction rates, polyp contraction rates and changes in the direction of gastrovascular flow is presented in Table 1 for both starved and newly fed colonies. A correlation coefficient of close to 1 would be expected if local polyp contractions alone drive the gastrovascular flow and/or stolon contraction, or if only stolon contractions drive the local gastrovascular flow, or *vice versa*. Although significant positive correlations were obtained for different variables, no simple 1:1 relationship existed between any two variables. Thus, the findings suggest that the stolonal contractions are not a simple function of local gastrovascular flow or polyp contractions.

Positive correlations between these variables are most frequently observed in starved colonies (Table 1). Feeding often led to obstruction of stolonal canals at different regions, where dense food materials blocked the gastrovascular flow. Clogged canals required 1–8 h to reopen. Of particular interest is the observation that stolon contractions continued in areas between two obstructions. This

Table 1. *Kendall tau correlation matrix for the rates of polyp contractions (PC), contractions of the proximal stolons bearing the polyp (S0C), contractions of the distal side-branched stolons without a polyp (S1C) and gastrovascular flow in the proximal (S0F) and distal (S1F) stolons*

Before	PC		S0C		S1C		S0F		S1F	
After	α	β	α	β	α	β	α	β	α	β
PC			0.51**	0.43**	–	–	–	0.37*	–	–
S0C	0.45*	–			–	–	–	0.72***	–	–
S1C	–	–	–	–			–	–	0.36*	–
S0F	–	–	0.47*	0.66*	–	–			0.36*	–
S1F	–	–	–	–	–	–	–	–		

The upper right half of the matrix represents correlations for the two clones (α, β) before feeding and the lower left half represents correlations for the same colonies after feeding.

Only the statistically significant correlations are given; $*P<0.05$; $**P<0.01$; $***P<0.001$.

$N=24$ for all 'before feeding' correlations.

After feeding, not all variables could be measured with certainty at all measurement intervals; hence, for PC, S0C and S0F, N is 16 (α) and 23 (β) and, for S1C, N is 19 and 24, respectively.

suggested that stolon contractions might persist in the absence of either polyp contractions or prevailing gastrovascular flow.

Contractions in isolated stolons

The contraction rates of isolated stolons of all four types tested did not differ significantly from the rates observed prior to their isolation ($P>0.05$, U-test; Fig. 5). In 9 of 12 such experiments, the isolated stolons grew back and fused to exactly the same point on the mother colony from which they had originally been separated. After fusion to the mother colony, the stolon contraction rate did not differ significantly from that measured for the stolon when isolated ($P>0.05$, U-test, Fig. 5). These findings suggested the existence of a mechanism for the control of stolonal contraction residing in the stolon itself.

The velocity of the gastrovascular flow in isolated stolons, however, was significantly lower than that observed in intact colonies. In another context we estimated the highest velocities of moving particles in the gastrovascular flow before and after separation of an S1 stolon from the colony. Based on the 10 highest values out of a total of 27 measurements, both before and after separation, the velocity decreased by a factor of six in an isolated stolon ($35.7\pm8.03\,\mu m\,s^{-1}$ in an intact S1 stolon compared to $6.0\pm1.03\,\mu m\,s^{-1}$ in the same isolated stolon).

Dimensions of ectoderm and endoderm during a contraction cycle

Measurements of the diameter of stolons, the lumen of the canal and the thickness of both the endoderm and the ectoderm were obtained from electron micrographs. The correlation matrix between these variables measured over a single contraction cycle is reported in Table 2. The only significant correlation was

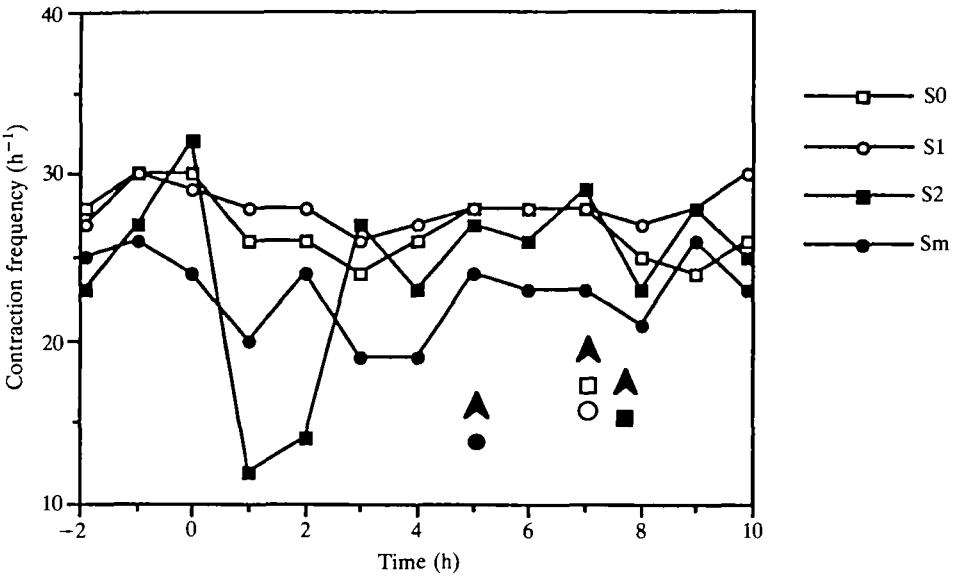

Fig. 5. A typical example of contractions in isolated stolons. The contraction frequencies of four different stolons of the same colony are given (S0, S1, S2, Sm, see Fig. 1). Stolons were completely disconnected from the colony at 0 h. The arrowheads mark the times at which isolated stolons had grown back and fused to the mother colony. Contraction rates were not significantly affected by vascular continuity with the mother colony.

Table 2. *Spearman correlation coefficients* (r_s) *for the canal diameter (CAN), stolon diameter (STO), endoderm thickness (END) and ectoderm thickness (ECT) at different stolon contraction stages along the same intact stolon*

	CAN	STO	END	ECT
Mean±S.D. (μm)	12.0±6.75	46.7±12.38	10.4±2.58	6.8±2.27
CAN	–	0.17	−0.72	−0.38
STO	P=0.61	–	0.22	0.03
END	P<0.01	P=0.4	–	0.34
ECT	P=0.22	P=0.93	P=0.29	–

Data are drawn from six different stolon cross sections (S1, clone β) measured from light microscopy photographs at 1000×.

Values of horizontal and vertical measurements have been pooled for the correlation analysis.

The canal size is the mean of the horizontal and the vertical canal diameters and the stolon diameter is measured exclusive of the periderm.

The only significant correlation exists between the canal diameter and the thickness of the endoderm.

The correlation coefficients are given in the upper right half and their statistical significances in the lower left half of the matrix.

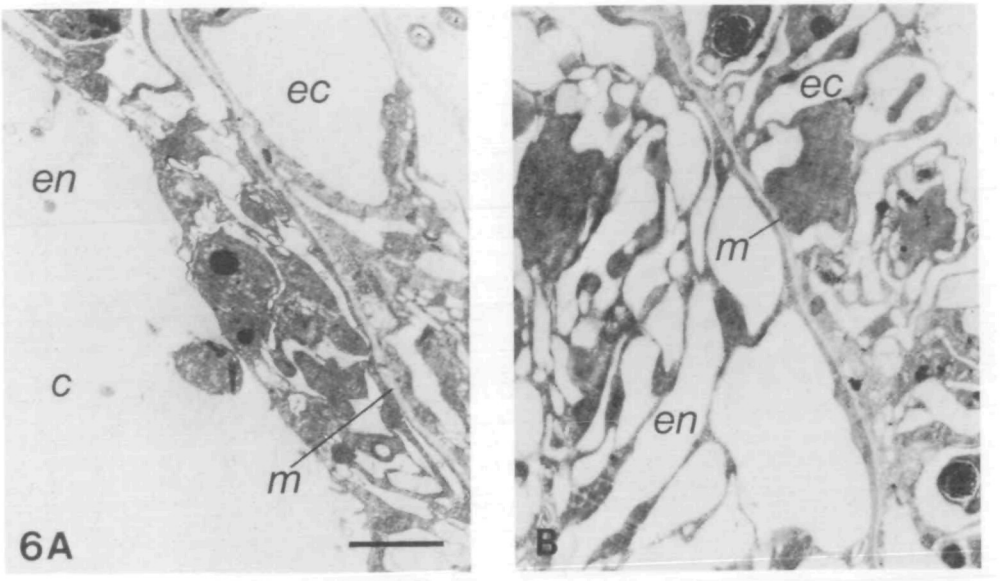

Fig. 6. Changes in endodermal volume during a contraction cycle. (A) Expanded stolon with compact, little-vacuolized endoderm; and (B) contracted stolon characterized by large, well-vacuolized endoderm; *c*, canal; *en*, endoderm; *ec*, ectoderm; *m*, mesoglea (light gray band). Scale bar, 2 μm.

a negative relationship between canal diameter and endoderm thickness, suggesting that the opening and closing of canals is associated with events unique to the endoderm (Fig. 6A,B, Table 2). Correlation coefficients relating the canal diameter to the thickness of the ectoderm and the stolon diameter were not significant, suggesting that although changes in the latter two occur they are not of primary importance for the stolon contraction–expansion cycles.

Transmission electron microscopy

Examination of cross sections in TEM from stolons in all stages of contraction revealed specialized, 'zipper-like' organelles (ZLOs). These organelles were found exclusively in apical portions of the endodermal cells, i.e. lining the lumen walls and the walls of the medial vacuoles (Fig. 7A). The ZLOs constituted approximately 2.5–3 % of the endodermal cytoplasm in these regions. At no time were ZLOs observed in basal portions of the endoderm or at any site in the ectoderm. Internally, the organelles consist of two parallel, electron-dense filaments (core) with numerous side arms radiating outwards towards the limiting membrane (Fig. 7B). No electron density was observed between the core filaments. The membrane-to-membrane separation was only 47 nm and the largest continuous ZLO was approximately 0.5 μm in length. The three-dimensional structure of the ZLO is unclear. Occasionally, circular cross sections were visible (Fig. 7A), suggesting a tubular structure. However, such cross sections were

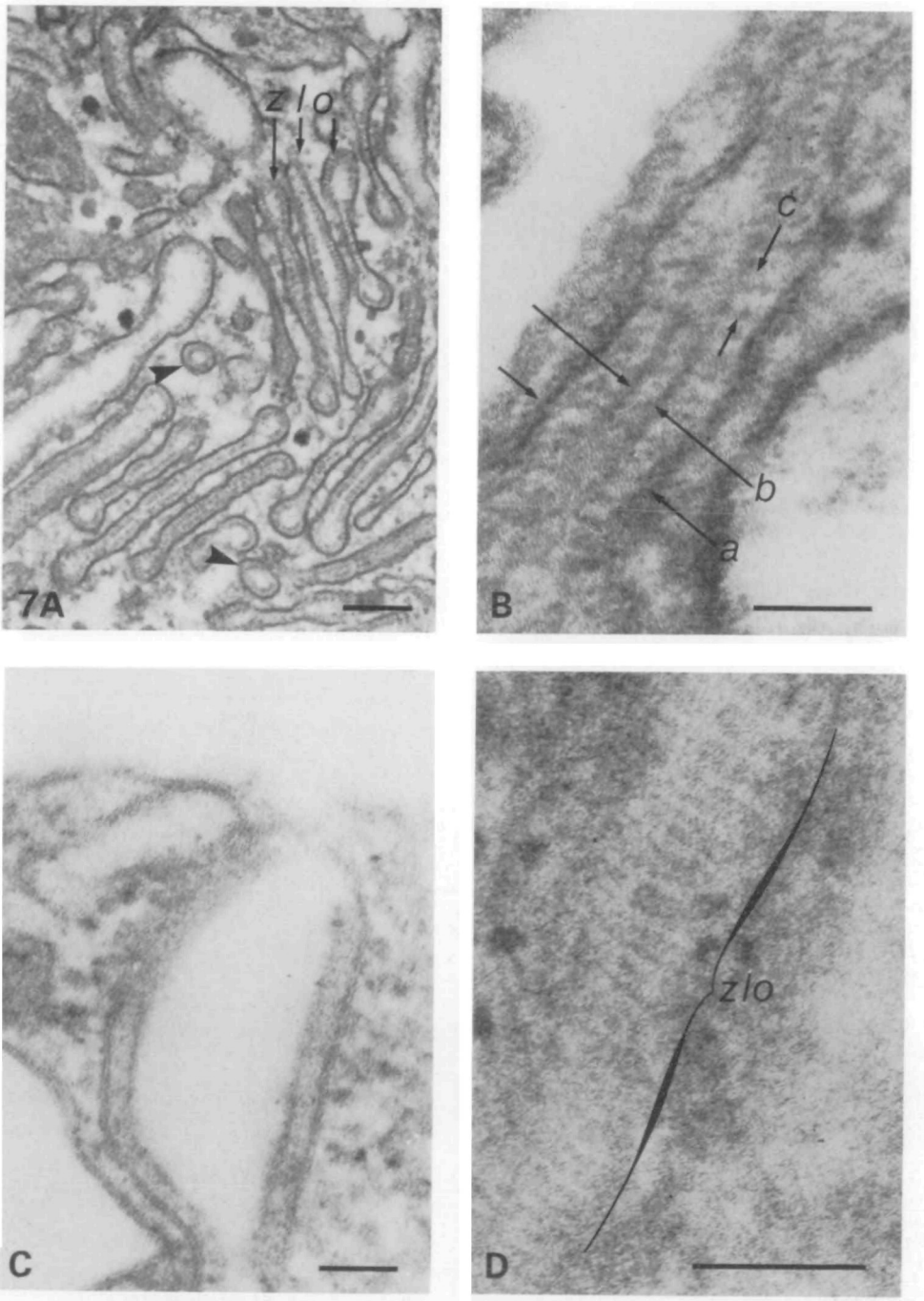

relatively rare and this suggests that the ZLO may exist in the form of large, flat sheets.

The appearance of ZLOs differed between stolon contraction stages. In cross sections of stolons fixed while undergoing the transition from the expanded to

Fig. 7. Zipper-like organelles (ZLO). (A) Survey micrograph of ZLOs in *Eleutheria dichotoma*. Scale bar, 0.1 μm. Circular cross sections (arrowheads), although readily visible in this micrograph, were not common. All other micrographs are from *Hydractinia symbiolongicarpus*. (B) Single ZLO. Scale bar, 50 nm. Average dimensions (means±1 S.E.): *a*, 47.8±1.91 nm; *b*, 10.9±0.63 nm; *c*, 9.4±0.63 nm. (C) Vacuolized ZLOs found in stolons undergoing the transition from the expanded to the contracted stage. Scale bar, 0.1 μm. As vacuolization occurs, internal morphology is lost. (D) Tangential section through wall of a vacuolized ZLO in a transitional-phase stolon. Note lengthening and pairing of side arms. Scale bar, 100 nm.

contracted state, vacuolized ZLOs were found. Here the central core filaments of ZLOs separated (Fig. 7C). Tangential sections through the walls of a vacuole reveal a lengthening and pairing of the side-arm filaments (Fig. 7D). In fully expanded and fully contracted stolons, the vacuolized ZLOs are largely absent. Endodermal cells of contracted stolons are characterized by extensive vacuolization and remnants of ZLOs may occasionally be seen (Figs 6B, 8B), whereas expanded stolons are characterized by few vacuoles in the endoderm (Fig. 6A).

The differences between cross sections taken at differing points in the stolonal expansion and contraction cycle are summarized in Table 3. Compact ZLOs with closed zippers are present in all stages of stolonal contraction. In contrast, vacuolized ZLOs occur at high frequency only in stolonal stages of transition

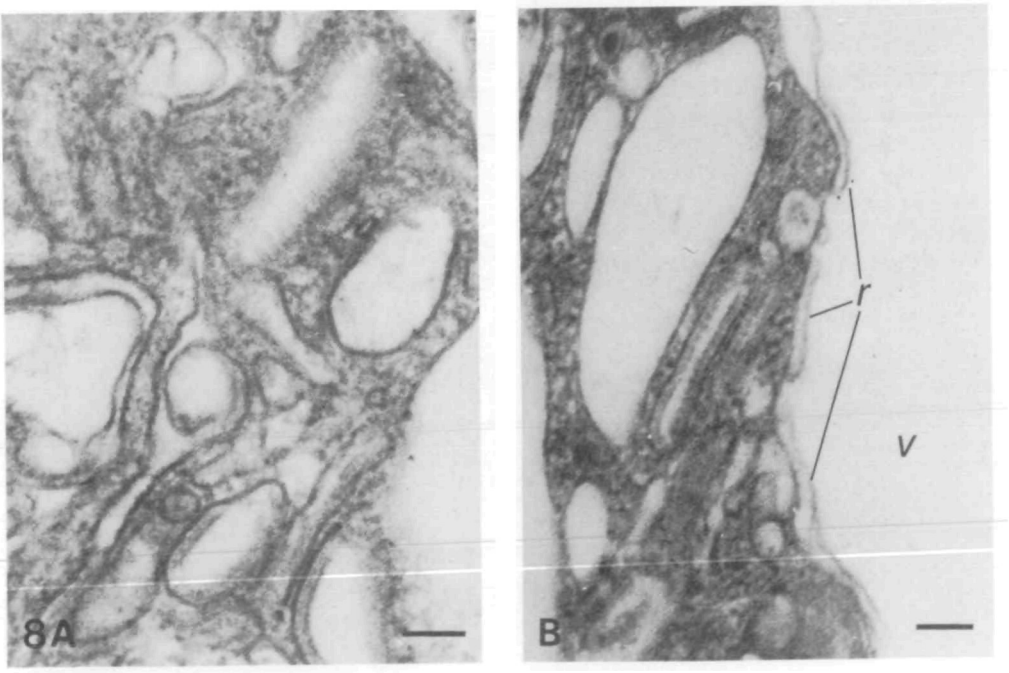

Fig. 8. (A) Survey micrograph of a stolon in the transitional phase showing a variety of ZLO conformations. Scale bar, 0.1 μm. (B) Greatly expanded vacuoles (*v*) in an almost contracted stolon with remnants (*r*) of the limiting membrane of the ZLO. Scale bar, 0.1 μm.

Table 3. *Fractional vacuole volumes and zipper-like organelle (ZLO) densities along an isolated stolon at different contraction stages (canal sizes 0–279 μm^2) and in a completely expanded stolon (canal size 1189 μm^2)*

	ZLO density		Fractional vacuole volume	
Canal size (μm^2)	Closed (no. per 15 μm^2)	Vacuolized (no. per 15 μm^2)	Endoderm (%)	Ectoderm (%)
1189	0.5±0.40	0.0±0.00	30	44
279	0.5±0.17	1.1±0.38	51	47
176	0.7±0.33	0.9±0.31	50	41
34	0.3±0.16	1.0±0.52	69	43
0	0.4±0.18	0.1±0.12	67	50

Values for the ZLO densities include only cytoplasmic area without vacuoles and each is derived from measurements of 8–10 different localities in a given cross section.

Values are presented as means±1 S.E.

Intercellular spaces are included in fractional vacuole volumes.

between expanded and contracted. A marked increase in endodermal cell vacuolization accompanies the transition stage and reaches a maximum during the stolonal contraction stage. Within different cross sections, the degree of ectodermal vacuolization was variable. However, no net change in ectodermal vacuolization accompanied the contraction cycle. Thus, differences in the appearance of ZLOs in the endoderm are correlated with vacuolization of the endoderm (Table 3), which is in turn correlated with the opening and closing of the gastrovascular canal (Table 2). ZLOs of an obviously identical ultrastructure were found also only in the stolonal endoderm of *Eleutheria dichotoma*.

Actin staining

Although epithelio-muscular cells have not previously been noted in hydroid stolons, Rhodamine–Phalloidin staining of intact stolons was performed to exclude the possibility of their occurrence in the stolons of *Hydractinia*. Rhodamine–Phalloidin bound to sites, i.e. F-actin, in all stolons and polyps of a colony. Binding patterns in polyps (not shown) showed extensive muscular elements, but no such structures were evident in stolons. In the stolons only the endoderm stained intensely. Diffuse actin staining was apparent almost throughout the expanded stolons (Fig. 9A,B), whereas staining was concentrated around the central canal, now closed by endoderm cells, in contracted stolons of the same colony (Fig. 9C,D). The pattern of actin-staining in the endoderm was consistent with the known distribution of ZLOs in the apical endoderm, and it is possible that

Fig. 9. Rhodamine–Phalloidin staining. (A) An expanded stolon in phase contrast. (B) Rhodamine–Phalloidin staining of actin of the same stolon as that in A in fluorescence light, marking actin filaments as white spots. (C) A contracted stolon in phase contrast. (D) Rhodamine–phalloidin staining of actin in the same stolon as that in C in fluorescent light. The stolon width is approximately 80 μm.

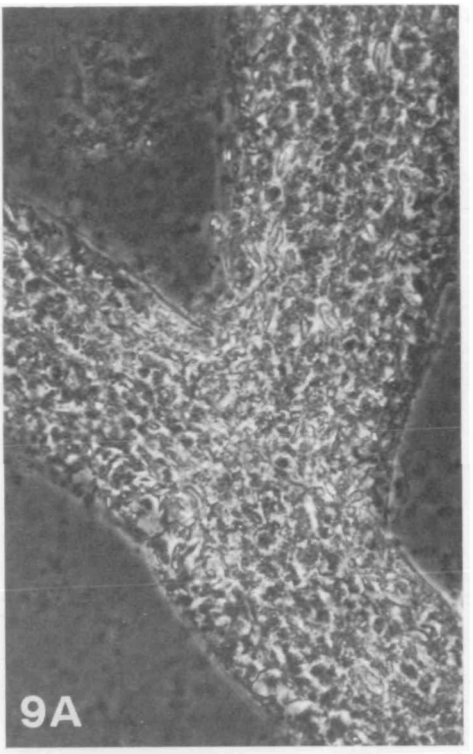
9A

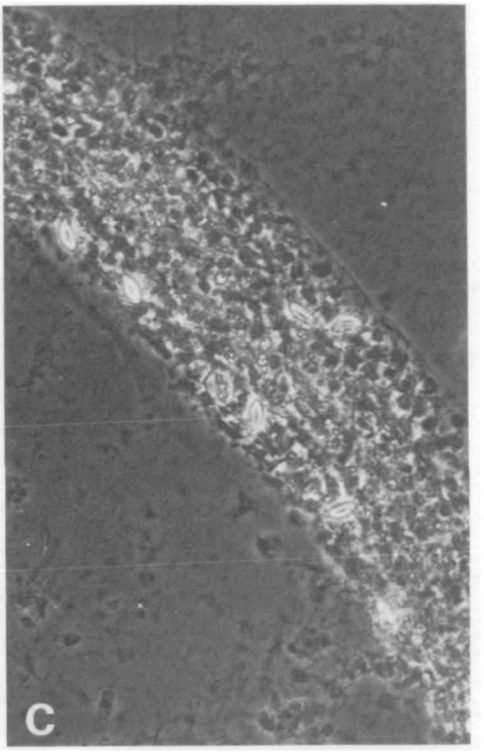
C

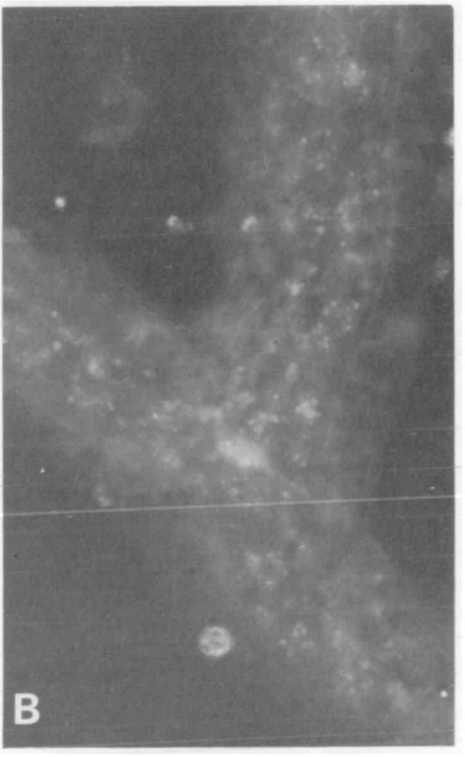
B

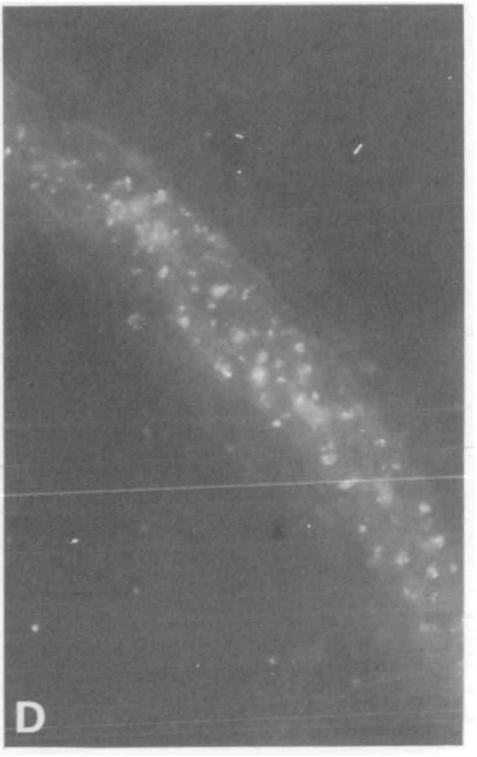
D

actin is associated with ZLO function. A decision on whether actin might be part of the membranes of the ZLOs, however, must await immunocytochemistry studies.

Discussion

The ZLO identified in transmission electron micrographs behaves in a fashion expected of a contractile vacuole. While TEM observations are necessarily static, the contractile nature of ZLOs may be inferred from differences in ZLO organization in the sequence of cross sections derived from stolons at three different stages in the dynamic process of stolonal contraction. In the expanded state, the stolon endoderm is characterized by few vacuoles and by no ZLOs of the vacuolized morphology. The appearance of the vacuolized ZLOs is coincident with the transition from stolonal expansion to contraction and an increase in the extent of endodermal vacuolization that occurs at this time (Tables 2, 3). Finally, in the contracted stolon state, endodermal vacuoles are large and fill most of the lumen of the endoderm cells and vacuolized ZLOs are almost absent (Tables 2, 3). These observations provide compelling evidence that the ZLO is a contractile vacuole.

This is the first report of such an organelle from a cnidarian. Amongst the metazoans, only sponges had previously been known to display contractile vacuoles (Gatenby *et al.* 1955; Brauer, 1975; Simpson, 1984). Contractile organelles are common in protists (Kitching, 1956; Patterson, 1980), where, as in sponges, they occur most frequently in freshwater forms. In these organisms, contractile vacuoles are presumed to function as intracellular pumps acting to maintain cell volume (Patterson, 1980). The ZLOs of *Hydractinia,* however, act in a different fashion. Rather than expelling water from intracellular stores to the external environment, these organelles act to absorb and release gastrovascular fluid from a common vascular lumen to which they show, at least temporarily, open connections. The ultrastructure of the contractile vacuole of *Hydractinia* and *Eleutheria* does not bear obvious structural similarity to the contractile vacuoles of protists and sponges (Patterson, 1980; Akbarieh and Couillard, 1988), and any inference as to evolutionary origins would be premature.

The function of these organelles may be threefold. The gastrovascular fluid is rich in solutes, providing for both respiration and nourishment. We speculate that the contractile vacuoles of *Hydractinia* act to facilitate both gas exchange and uptake of dissolved organic material from the gastric vasculature. The so-called 'rod-shaped' or 'cytoplasmic' vesicles in *Hydra* (Burnett, 1973) are probably the same organelles as the ZLOs described here. These vesicles have been described as phagocytotic, and as adding reversibly to the apical surface membrane of the endoderm (gastrodermis) and also as fusing to larger 'digestive' vacuoles (Burnett, 1973). These findings nicely complement our interpretation of ZLOs playing an important role in feeding, i.e. in the uptake and release of gastrovascular fluid from and into the stolonal canals. The question of whether the ZLOs and all larger

endodermal vacuoles might be different members of the same population of vesicles cannot be answered at present. However, this study shows that ZLOs probably fulfill two additional functions, independently of their role in feeding. A second function is evident from the observation that ZLO vacuolization acts to close the canal lumen and, hence, to block local gastrovascular flow. Thus, contractile-vacuole-mediated stolon contractions may serve to regulate the spatial and temporal distribution of gastrovascular flow within a colony. Such a mechanism is of particular importance in a vascular system in which a single canal is utilized for both afferent and efferent flow. A third function is evident from our observations of isolated stolons. It is clear from these experiments that the activity of contractile vacuoles is sufficient to initiate and maintain limited gastrovascular flow.

Although stolonal contractions are capable of supporting gastrovascular flow, they are unlikely to provide the main force driving gastrovascular flow in intact colonies, as shown by our observation that the velocity of gastrovascular flow in the absence of polyps is substantially reduced relative to that measured in an intact colony. Karlson and Marferin (1984) have shown that gastrovascular flow can be strongly influenced by the cumulative effect of polyp contractions at sites in the colony distant from the point observed. Under these conditions, only weak correlations may be found between local polyp contraction and local gastrovascular flow (Table 1). If the main gastrovascular flow is propelled by polyp contraction (Karlson and Marferin, 1984; Marferin, 1985), then stolons would generally stay under high gastrovascular fluid pressure generated by distant polyps. This pressure might support a passive inflow into the contractile vacuoles (diastole) during stolonal contraction. As gastrovascular flow is diverted to other regions of the colony and local pressure drops, the contractile vacuole probably contracts (systole) and releases gastrovascular fluid into the gastric system to generate stolonal expansion. It seems likely that forces due to the elasticity of the epithelia and the mesoglea relative to the antagonistic, inelastic periderm also play a role in stolon expansion. The time courses for stolon expansion and contraction phases, as well as Hale's (1960) observation that the resting state of the stolon in an anesthetized colony is the contracted state, suggest that stolon expansion, i.e. emptying of the contractile vacuoles, is the active phase. Thus, contractile vacuoles may not serve as important forces driving gastrovascular flow, but may play an important role in directing gastrovascular flow by opening and blocking stolonal canals reversibly in response to local pressure differentials (Fig. 10).

Contractile-vacuole-mediated stolon contractions may also bear on the mechanisms of stolon formation in growing colonies. It has been demonstrated that stolon tips can be evoked by mechanical pressure in regions of the colony competent to form stolons (Plickert, 1980; Müller and Plickert, 1982; Müller *et al.* 1987), as well as by chemical and electrical signals (Müller and El-Shershaby, 1981; Müller *et al.* 1987). The pattern of stolon contractions in the area of a branching event can, in principle, provide a temporary increase in gastrovascular pressure to drive out the new stolon, by regulating the diameter of canal openings or by regulating the

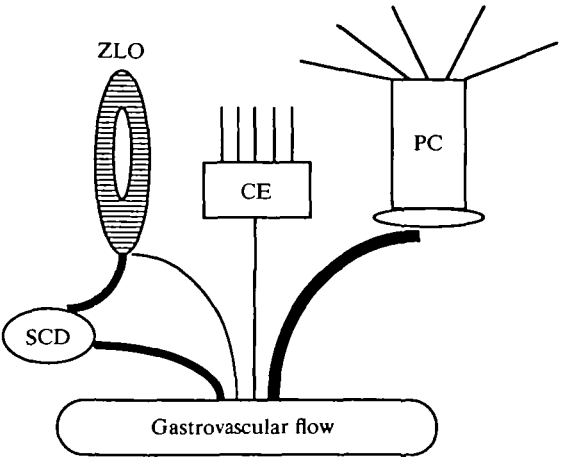

Fig. 10. Factors responsible for control of the stolonal gastrovascular flow. The polyp contractions (PC) generate high pressure in the gastrovascular fluid and provide the main driving force for the gastrovascular flow. The ciliated endoderm cells (CE) serve to agitate particles in the stream, but do not drive gastrovascular flow (Berrill, 1949; Hale, 1960). The contractile stolonal vacuoles (ZLO) affect the gastrovascular flow in two ways: (1) directly, by periodically absorbing and releasing gastrovascular fluid, and (2) indirectly, by periodically changing the stolonal canal diameter (SCD) and hence opening or closing the endodermal canals for the gastrovascular flow. The latter allows the creation of complex and variable local flow patterns within the colony. Thus, at the same time, different stolonal regions can show different flow patterns with respect to velocity and direction, while the total volume and pressure in the system of a whole colony can be kept constant.

timing of canal opening. The tip region of an outgrowing stolon is a blind end, and hence the diameter of the opening of a canal leading from a main stolon to a tip should determine the hydrodynamic pressure on the tip and, in turn, influence the extent of forward deformation of the tip (Wyttenbach, 1973; Beloussov *et al.* 1989). Given the lack of nerve cells in stolons, such an effect might be coordinated by a fast epithelial conducting system (Josephson, 1961; Mackie, 1973; Stokes, 1974*a*,*b*) acting to control stolon contraction patterns. An epithelial conducting system has been suggested to be present in hydroid stolons on the basis of ultrastructural evidence (Overton, 1963). The role of stolon contractions in mediating stolon tip formation bears further investigation.

Our observations confirm and extend several observations made by prior investigators. As both Berrill (1949) and Hale (1960) independently observed for *Obelia commissularis* and *Clytia johnstoni*, respectively, we find that stolon contractions and gastrovascular flow are sustained in the absence of polyps (Fig. 4). Further, Hale (1960) had observed that stolonal contractions are accompanied by large changes in the volume of endodermal cells without comparable changes in the dimensions of the ectoderm (Table 2). In particular,

Berrill has noted that in *Obelia* specialized regions of the stolon are characterized by extensive endodermal vacuolization. Hudson (1965) subsequently showed that these vacuolized regions are contractile in nature. The correspondence between our findings and the observations made on different hydroids suggests that the contractile vacuoles identified in *Hydractinia* may be characteristic of the vascular system of hydroids.

Finally, our results bear directly on the study of growing tips. Growing tips are specialized regions of stolons that are said to 'pulsate' (Wyttenbach, 1968, 1973, 1974; Crowell, 1974; Beloussov *et al.* 1989), and changes in the shape of the tip region have been attributed to periodic changes in the extent of vacuolization of the tip ectoderm (Beloussov *et al.* 1989). ZLOs, however, occur in the tip endoderm (and not in the ectoderm) in *Hydractinia* and *Eleutheria*, suggesting that changes in the endoderm may also play a role in tip growth. Since the endoderm of the stolonal tip is also highly vacuolated (see Fig. 5 in Beloussov *et al.* 1989) and since Donaldson (1974) has shown that tip pulsations are blocked by cytochalasin B, it seems likely that the extent of tip elongation is a joint consequence of ectodermal and endodermal vacuolization.

The following predictions can be made if the suggested model for the function of stolonal contractions presented here is correct. (1) If the contractile- vacuole-mediated stolon contractions depend upon an active metabolic process, a shortage of ATP (induced experimentally by inhibitors of mitochondrial functions, Blackstone, 1990, or naturally by low oxygen concentrations in the environment) should slow stolon expansion. (2) If nourishment is an important function of stolonal contractions, colony growth rates should follow a sigmoidal temperature dependency similar to that of stolon contraction frequencies. (3) Fast-growing stolons should show high contraction frequencies and/or large contraction amplitudes. (4) S0 stolons, which are directly connected to a polyp, should have faster growth rates than S1 and S2 stolons. (5) Poorly nourished regions in a larger colony should have relatively more closed stolons, favouring growth in the better nourished regions; i.e. stolon contractions are affected by a positive feedback mechanism. Those stolons growing fast and contracting frequently will be nourished at the expense of slower-growing stolons; consequently, regions of clearly different growth rates should be found at any given time within one colony. These predictions will be tested and used for experimental manipulations in further studies.

Supported by DFG (III-02-Schi-277/1-1), NSF (BSR-88-05961, DCB-90-18003, OCE-90-18396) and ONR (N00014-89-J-3046). We thank L. Beloussov, N. Blackstone, D. Bridge, C. Cunningham, M. Dick, C. Hauenschild, H. Hadrys, M. Max and M. Peterson for comments on the manuscript and J. Taschner for technical assistance. This paper is dedicated to Professor Carl Hauenschild on the occasion of his 65th birthday and retirement as Professor Emeritus from the chair of zoology at Braunschweig University.

References

AKBARIEH, M. AND COUILLARD, P. (1988). Ultrastructure of the contractile vacuole and its periphery in *Amoeba proteus*: Evolution of vesicles during the cycle. *J. Protozool.* **35**, 99–108.

BELOUSSOV, L. V., LABAS, J. A., KAZAKOVA, N. I. AND ZARAISKY, A. G. (1989). Cytophysiology of growth pulsations in hydroid polyps. *J. exp. Zool.* **249**, 258–270.

BERRILL, N. J. (1949). The polymorphic transformations of *Obelia*. *Q. Jl microsc. Sci.* **90**, 235–254.

BLACKSTONE, N. W. (1990). Heterochrony in hydractiniid hydroids: a hypothesis. In *Principles of Organization in Organisms. SFI Studies in the Sciences of Complexity*, vol. XII (ed. A. Boskin and J. Mittenthal). Reading, MA: Addison-Wesley (in press).

BRAUER, E. B. (1975). Osmoregulation in the fresh water sponge, *Spongilla lacustris*. *J. exp. Zool.* **192**, 193–202.

BURNETT, A. L. (1973). *Biology of* Hydra, pp. 50–56. New York, London: Academic Press.

BUSS, L. W. AND YUND, P. O. (1988). A comparison of modern and historical populations of the colonial hydroid *Hydractinia*. *Ecology* **69**, 646–654.

BUSS, L. W. AND YUND, P. O. (1989). A sibling species group of *Hydractinia* in the northeastern United States. *J. mar. biol. Ass. U.K.* **69**, 857–875.

COSSINS, A. R. AND BOWLER, K. (1987). *Temperature Biology of Animals*. London, New York: Chapman and Hall.

CROWELL, S. (1974). Morphogenetic events associated with stolon elongation in colonial hydroids. *Am. Zool.* **14**, 665–672.

DONALDSON, S. (1974). Terminal motility in elongating stolons of *Proboscidactyla flavicirrata*. *Am. Zool.* **14**, 735–744.

FAULSTICH, H., ZOBELEY, S., RINNERTHALER, G. AND SMALL, J. V. (1988). Fluorescent phallotoxins as probes for filamentous actin. *J. Musc. Res. cell. Motility* **9**, 370–383.

FULTON, C. (1963). Rhythmic movements in *Cordylomorpha*. *J. cell. comp. Physiol.* **61**, 39–51.

GATENBY, J. B., DALTON, A. J. AND FELIX, M. D. (1955). The contractile vacuole of Parazoa and Protozoa, and the Golgi apparatus. *Nature* **176**, 301–302.

HALE, L. J. (1960). Contractility and gastrovascular movements in the hydroid *Clytia johnstoni*. *Q. Jl microsc. Sci.* **101**, 339–350.

HALE, L. J. (1964). Cell movements, cell division and growth in the hydroid *Clytia johnstoni*. *J. Embryol. exp. Morph.* **12**, 517–538.

HAMMETT, F. S. AND PADIS, N. (1935). Correlation between developmental status of *Obelia* hydranths and direction of gastrovascular streaming within their pedicils. *Protoplasma* **23**, 81–85.

HAUENSCHILD, C. (1954). Genetische und entwicklungsphysiologische Untersuchungen über Intersexualität und Gewebeverträglichkeit bei *Hydractinia echinata* Flemm. (Hydroz. Bougainvill.) *Wilhelm Roux Arch. EntwMech.* **147**, 1–41.

HAUENSCHILD, C. (1956). Experimentelle Untersuchungen über die Entstehung asexueller Klone bei der Hydromeduse *Eleutheria dichotoma*. *Z. Naturf.* **11b**, 394–402.

HAUSCHKA, T. (1944). The role of gastrovascular pressure in hydroid growth. *Growth* **8**, 321–336.

HUDSON, R. C. L. (1965). A new contractile region in the stolon of the hydroid *Clytia johnstoni*. *Biol. J. (Univ. St Andrews)* **5**, 14–23.

HUXLEY, J. S. AND DEBEER, G. R. (1923). Studies in dedifferentiation. IV. Resorption and differential inhibition in *Obelia* and *Campanularia*. *Q. Jl microsc. Sci.* **67**, 473–494.

JOSEPHSON, R. K. (1961). Colonial responses of hydroid polyps. *J. exp. Biol.* **38**, 559–577.

KARLSON, A. G. AND MARFERIN, N. N. (1984). Movements of gastrovascular fluid in the colony of the hydroid *Dynamena pumila* and some other species. *J. obsch. Biol.* **45**, 670–679.

KITCHING, J. A. (1956). Contractile vacuoles of Protozoa. *Protoplasma* **3**, 1–45.

MACKIE, G. O. (1973). Coordinated behavior in hydrozoan colonies. In *Animal Colonies* (ed. R. S. Boardman, A. H. Cheetam and W. A. Oliver), pp. 95–106. Stroudsburg, PA: Dowden, Hutchinson.

MARFERIN, N. N. (1985). The functioning of the pulsatory–peristaltic type transport system in colonial hydroids. *J. gen. Biol.* **46**, 153–164.

MCFADDEN, C. S., MCFARLAND, M. AND BUSS, L. W. (1984). Biology of hydractiniid hydroids.

I. Colony ontogeny in *Hydractinia echinata*. *Biol. Bull. mar. biol. Lab., Woods Hole* **166**, 54–67.

MÜLLER, W. A. (1974). *Hydractinia echinata* (Hydrozoa). Organisation des Stockes, Nahrungsaufnahme. *Inst. Wiss. Film. Goettingen* **E 2079**, 3–11.

MÜLLER, W. A. (1975). *Hydractinia echinata* (Hydrozoa). Ablaichen, Embryonalentwicklung, Metamorphose. *Inst. Wiss. Film. Goettingen* **E 2080**, 3–16.

MÜLLER, W. A. AND EL-SHERSHABY, E. (1981). Electrical current and cAMP induce lateral branching in the stolon of hydroids. *Devl Biol.* **87**, 24–29.

MÜLLER, W. A., HAUCH, A. AND PLICKERT, G. (1987). Morphogenetic factors in hydroids. I. Stolon tip activation and inhibition. *J. exp. Zool.* **243**, 111–124.

MÜLLER, W. A. AND PLICKERT, G. (1982). Quantitative analysis of an inhibitory gradient field in the hydrozoan stolon. *Wilhelm Roux Arch. EntwMech.* **191**, 56–63.

OVERTON, J. (1963). Intercellular connections in the outgrowing stolon of *Cordylophora*. *J. Cell Biol.* **17**, 661–671.

PATTERSON, D. J. (1980). Contractile vacuoles and associative structures: Their organization and function. *Biol. Rev.* **55**, 1–46.

PLICKERT, G. (1980). Mechanically induced stolon branching in *Eirene viridula* (Thecta, Companulinidae). In *Developmental and Cellular Biology of Coelenterates* (ed. P. Tardent and R. Tardent), pp. 185–190. Amsterdam, New York, Oxford: Biomedical Press.

PRECHT, H., CHRISTOPHERSEN, J., HENSEL, H. AND LARCHER, W. (1973). *Temperature and Life*. Berlin, Heidelberg, New York: Springer.

SCHIERWATER, B. (1989). Allometric changes during growth and reproduction in *Eleutheria dichotoma* (Hydrozoa, Athecata) and the problem of estimating body size in a microscopic animal. *J. Morph.* **200**, 255–267.

SIMPSON, T. L. (1984). *The Cell Biology of Sponges*, pp. 67–69. Berlin, Heidelberg, New York, Tokyo: Springer.

STOKES, D. R. (1974*a*). Physiological studies of conducting systems in colonial hydroid *Hydractinia echinata*. I. Polyp specialization. *J. exp. Zool.* **190**, 1–18.

STOKES, D. R. (1974*b*). Morphological substrates of conduction in colonial hydroid *Hydractinia echinata*. I. Ectodermal nerve net. *J. exp. Zool.* **190**, 19–45.

WYTTENBACH, C. R. (1968). The dynamics of stolon elongation in the hydroid *Campanularia flexuosa*. *J. exp. Zool.* **167**, 333–352.

WYTTENBACH, C. R. (1973). The role of gastrovascular pressure in stolonic growth movements in the hydroid, *Bougainvilla*. *J. exp. Zool.* **186**, 79–90.

WYTTENBACH, C. R. (1974). Cell movements associated with terminal growth in colonial hydroids. *Am. Zool.* **14**, 699–717.